

## Article

# Identification and Expression of the *MADS-box* Gene Family in Different Versions of the *Ginkgo biloba* Genome

Pengyan Zhou <sup>1,2</sup> , Zesen Wang <sup>2</sup>, Yingang Li <sup>1</sup>  and Qi Zhou <sup>1,\*</sup> 

<sup>1</sup> Zhejiang Academy of Forestry, 399 Liuhe Road, Hangzhou 310023, China; pyzhou@njfu.edu.cn (P.Z.); hzliy@126.com (Y.L.)

<sup>2</sup> Co-Innovation Center for Sustainable Forestry in Southern China, Nanjing Forestry University, Nanjing 210037, China; wzs158159@163.com

\* Correspondence: qizhou36@hotmail.com; Tel.: +86-0571-87798072

**Abstract:** *MADS-box* transcription factors play important roles in many organisms. These transcription factors are involved in processes such as the formation of the flower organ structure and the seed development of plants. *Ginkgo biloba* has two genome versions (version 2019 and version 2021), and there is no analysis or comparison of the *MADS-box* gene family in these two genomes. In this study, 26 and 20 *MADS-box* genes were identified from the two genomes of *Ginkgo*, of which 12 pairs of genes reached more than 80% similarity. According to our phylogenetic analysis results, we divided these genes into type I (*Mα* and *Mγ* subfamilies) and type II (*MIKC* and *Mδ* subfamilies) members. We found that both sets of genomes lacked the *Mβ* gene, while the *MIKC* gene was the most numerous. Further analysis of the gene structure showed that the *MIKC* genes in the two genomes had extralong introns ( $\geq 20$  kb); these introns had different splicing patterns, and their expression might be more abundant. The gene expression analysis proved that *GbMADS* genes were expressed to varying degrees in eight *Ginkgo* biological tissues. Type II *GbMADS* genes not only were found to be related to female flower bud differentiation and development but also are important in seed development. Therefore, *MADS-box* genes may play important roles in the development of *Ginkgo* reproductive organs, which may suggest a genetic role in sexual differentiation. This study further contributes to the research on *MADS-box* genes and provides new insights into sex determination in *Ginkgo*.

**Keywords:** *Ginkgo* genome; *MADS-box*; gene structure; expression



**Citation:** Zhou, P.; Wang, Z.; Li, Y.; Zhou, Q. Identification and Expression of the *MADS-box* Gene Family in Different Versions of the *Ginkgo biloba* Genome. *Plants* **2023**, *12*, 3334. <https://doi.org/10.3390/plants12183334>

Academic Editor: Young Hee Joung

Received: 14 August 2023

Revised: 13 September 2023

Accepted: 18 September 2023

Published: 21 September 2023



**Copyright:** © 2023 by the authors. Licensee MDPI, Basel, Switzerland. This article is an open access article distributed under the terms and conditions of the Creative Commons Attribution (CC BY) license (<https://creativecommons.org/licenses/by/4.0/>).

## 1. Introduction

*MADS-box* gene family members encode transcription factors (TFs), which play an important role in many biological functions in eukaryotes [1]. *MADS-box* TFs are characterized by the presence of a DNA-binding domain of approximately 60 amino acids (aa) in length, which is collectively called the MADS domain. This domain was located in the N-terminal region of the protein. One of the most notable features of *MADS-box* gene family members is their important role in the flowering ABCDE model of plants [2]. Researchers have conducted many studies in *Arabidopsis thaliana*, *Oryza sativa* L., *Populus* L., etc. [3–5]. The *MADS-box* gene has been shown to be critical in regulating plant development, for example, in female gametophytes, seed development, and fruit ripening [6]. It was reported that *MADS-box* genes also participate in responses to stress, both abiotic and biotic stress [7]. For example, the expression of *TaMADS2* is upregulated after wheat stripe rust infection [8], and some *MADS-box* genes might also be involved in responses to high salt concentrations [9]. In addition, recent progress that has been made regarding the roles of *MADS* genes during gymnosperm reproduction deserves more attention. *MADS11* and *DAL1* interact to mediate the vegetative-to-reproductive transition in pine [10]. The male-specific region of the Y chromosome of *Cycas* contains a *MADS-box* transcription

factor expressed exclusively in male cones [11]. These studies have important implications for *MADS-box* genes in gymnosperms.

Gramzow et al. classified the *MADS-box* genes into SRF-like (type I) and MEF2-like (type II) [12]. Type I included type M and type N genes [13]. In addition to the MADS domain (M), type II genes contain three additional domains, namely, an intervening domain (I), a keratin-like domain (K), and a C-terminal domain (C). Type II genes can be divided into MIKC<sup>C</sup> and MIKC\* genes according to their structural differences [4,14]. Bayesian classification of MADS-box proteins in *A. thaliana* clustered the proteins into five distinct groups (M $\alpha$ , M $\beta$ , M $\gamma$ , M $\delta$ , and MIKC) [3]. This classification scheme was used in this study.

*Ginkgo biloba*, which is native to China, is the only species in the Ginkgo family [15]. Ginkgo fruit has antioxidant, antibacterial, and other biological functions [16]. Ginkgo is a typical hermaphroditic plant species, and there are great differences in the application of the different sexes. Female plants are mostly used for fruit production. However, due to the unpleasant smell of ripe fruit, male plants tend to be chosen for landscaping. In theory, it takes 20 to 30 years for the sex of Ginkgo seedlings to be identified according to the inflorescence, which greatly limits the promotion and application of different sexes of Ginkgo trees. Therefore, exploring the mechanism of sex differentiation in Ginkgo has become a research priority. The MADS-box gene plays an important role in flower bud differentiation, while its role in Ginkgo sex regulation remains unknown. Although the *MADS-box* gene family was initially identified in Ginkgo [17], the Ginkgo genome has been published in two versions. In 2019, Guan et al. updated the Ginkgo genome assembly to the chromosome level with Hi-C technology and obtained a high-quality Ginkgo genome [18]. In 2021, Liu et al. presented another Ginkgo genome assembly based on long reads (PacBio RSII platform) [19]. Considering the incomplete assembly of genomes and the possibility of annotation errors, it is particularly important to compare the differences in *MADS-box* genes between the two genomes.

Although a small number of *MADS-box* genes have also been verified in Ginkgo [20–22], genome-wide identification and expression analysis from two genomes is still lacking. Studies have shown that genome duplication events often lead to an increase in gene family members and redundancy in function. Ginkgo has experienced only one duplication event common to the ancestors of seed-bearing plants (~320 Mya) [19,23]. Considering the information in the iTAK database [24], the Ginkgo TF families usually have relatively few members. Therefore, studies of the function of family members tend to be representative of the species.

In this study, we comprehensively identified the *MADS-box* gene family of Ginkgo from a genome-wide perspective. For the first time, we mined MADS genes from two Ginkgo genomes simultaneously. We wanted to determine the differences in Ginkgo MADS genes in the two genomes and to analyze their structural characteristics. Through a quantitative expression analysis of the *MADS-box* gene in eight different tissues, we tried to comprehensively explore the potential function of the *MADS-box* genes in various tissues of Ginkgo. This study provides the first expression study of *MADS-box* genes within two Ginkgo genomes and has given a different idea for molecular biology research on Ginkgo.

## 2. Results

### 2.1. Identification of GbMADS Proteins

According to the results of BLAST and HMM models, 40 GbMADS candidates were initially detected throughout the version 2019 genome (v2019), and 28 candidates were initially detected throughout the version 2021 genome (v2021); their protein sequences are shown in Supplementary S1 and S2, respectively. Based on the MADS-box model in the SMART program, 26 proteins and 20 proteins with complete MADS-box domains were identified in v2019 and v2021, respectively (Table 1). In order to distinguish them, the 2019 version is named as GbMADS1-GbMADS26 and the 2021 version is named as GbMADS27-GbMADS46. Among them, there were 12 pairs of genes that reached 80% similarity. They all have a conserved MADS domain consisting of approximately 60 aa,

which is located at the N-terminus. Multisequence alignment and the sequence icon of MADS domains v2019 revealed 10 highly conserved aa (17, 21, 23, 24, 27, 30, 31, 34, 35, and 39). In contrast, the MADS domains v2021 revealed 13 highly conserved aa (1, 2, 17, 21, 23, 24, 27, 30, 31, 34, 38, 39, 48) (Figure S1).

**Table 1.** Physicochemical properties and intron information of GbMADS.

| Gene Name           | Sequence ID    | Length (aa) | MW (kDa)  | pI    | GRAVY  | Subcellular Localization | Type | Intron |
|---------------------|----------------|-------------|-----------|-------|--------|--------------------------|------|--------|
| <b>Version 2019</b> |                |             |           |       |        |                          |      |        |
| GbMADS01            | Gb_31417       | 381         | 43,295.54 | 5.96  | −0.672 | Nucleus                  | Mδ   | 10     |
| GbMADS02            | Gb_38365       | 134         | 15,267.48 | 9.34  | −0.480 | Nucleus                  | MIKC | 2      |
| GbMADS03            | Gb_41549       | 245         | 28,348.38 | 9.61  | −0.754 | Nucleus                  | MIKC | 7      |
| GbMADS04            | Gb_41550       | 201         | 22,539.02 | 9.28  | −0.051 | Nucleus                  | MIKC | 2      |
| GbMADS05            | Gb_36364       | 404         | 46,738.33 | 9.32  | −0.733 | Nucleus                  | MIKC | 7      |
| GbMADS06            | Gb_30604       | 166         | 19,373.46 | 10.20 | −0.710 | Nucleus                  | MIKC | 5      |
| GbMADS07            | Gb_38922       | 165         | 18,369.30 | 9.37  | 0.131  | Nucleus                  | MIKC | 1      |
| GbMADS08            | Gb_01884       | 372         | 42,803.94 | 9.66  | −0.272 | Nucleus                  | MIKC | 9      |
| GbMADS09            | Gb_19178       | 246         | 28,197.98 | 6.26  | −0.594 | Nucleus                  | MIKC | 7      |
| GbMADS10            | Gb_39109       | 199         | 22,576.68 | 6.22  | −0.513 | Nucleus                  | MIKC | 5      |
| GbMADS11            | Gb_38883       | 445         | 50,951.76 | 5.93  | −0.667 | Nucleus                  | My   | 1      |
| GbMADS12            | Gb_28587       | 257         | 29,385.11 | 9.90  | −0.416 | Nucleus                  | MIKC | 8      |
| GbMADS13            | Gb_05359       | 439         | 49,658.40 | 4.70  | −0.653 | Nucleus                  | My   | 3      |
| GbMADS14            | Gb_33168       | 209         | 24,345.65 | 5.53  | −0.708 | Nucleus                  | My   | 0      |
| GbMADS15            | Gb_12778       | 91          | 10,584.23 | 9.76  | −0.693 | Nucleus                  | MIKC | 2      |
| GbMADS16            | Gb_19258       | 336         | 37,202.07 | 8.33  | −0.704 | Nucleus                  | Mα   | 0      |
| GbMADS17            | Gb_03807       | 190         | 20,981.41 | 10.05 | −0.104 | Nucleus                  | MIKC | 5      |
| GbMADS18            | Gb_05128       | 412         | 47,476.12 | 6.33  | −0.385 | Nucleus                  | MIKC | 9      |
| GbMADS19            | Gb_03068       | 162         | 18,422.89 | 9.96  | −0.608 | Nucleus                  | MIKC | 3      |
| GbMADS20            | Gb_16301       | 380         | 43,797.09 | 8.93  | −0.226 | Nucleus                  | MIKC | 8      |
| GbMADS21            | Gb_12586       | 356         | 40,514.41 | 6.32  | −0.650 | Nucleus                  | Mα   | 0      |
| GbMADS22            | Gb_21526       | 169         | 19,411.53 | 10.17 | −0.499 | Nucleus                  | Mα   | 0      |
| GbMADS23            | Gb_15398       | 277         | 31,889.43 | 8.886 | −0.405 | Nucleus                  | MIKC | 7      |
| GbMADS24            | Gb_40092       | 336         | 37,284.17 | 8.33  | −0.680 | Nucleus                  | Mα   | 0      |
| GbMADS25            | Gb_37613       | 336         | 37,284.17 | 8.33  | −0.680 | Nucleus                  | Mα   | 0      |
| GbMADS26            | Gb_12581       | 122         | 13,740.90 | 10.02 | −0.397 | Nucleus                  | MIKC | 2      |
| <b>Version 2021</b> |                |             |           |       |        |                          |      |        |
| GbMADS27            | GWHPBAVD000173 | 451         | 51,348.86 | 5.61  | −0.562 | Nucleus                  | Mδ   | 12     |
| GbMADS28            | GWHPBAVD000308 | 67          | 7532.78   | 10.58 | −0.194 | Nucleus                  | MIKC | 1      |
| GbMADS29            | GWHPBAVD001358 | 252         | 29,170.87 | 8.88  | −0.917 | Nucleus                  | MIKC | 7      |
| GbMADS30            | GWHPBAVD001363 | 61          | 6849.08   | 10.21 | −0.292 | Nucleus                  | MIKC | 0      |
| GbMADS31            | GWHPBAVD001364 | 245         | 28,348.38 | 9.61  | −0.754 | Nucleus                  | MIKC | 7      |
| GbMADS32            | GWHPBAVD001372 | 61          | 6881.08   | 10.29 | −0.461 | Nucleus                  | MIKC | 0      |
| GbMADS33            | GWHPBAVD001859 | 445         | 50,951.76 | 5.93  | −0.667 | Nucleus                  | My   | 1      |
| GbMADS34            | GWHPBAVD009827 | 257         | 29,385.11 | 9.9   | −0.416 | Nucleus                  | MIKC | 8      |
| GbMADS35            | GWHPBAVD009828 | 221         | 25,387.11 | 9.73  | −0.666 | Nucleus                  | MIKC | 6      |
| GbMADS36            | GWHPBAVD009829 | 234         | 26,706.47 | 9.26  | −0.601 | Nucleus                  | MIKC | 7      |
| GbMADS37            | GWHPBAVD012282 | 209         | 24,345.65 | 5.53  | −0.708 | Nucleus                  | My   | 0      |
| GbMADS38            | GWHPBAVD018550 | 64          | 7293.57   | 10.09 | −0.169 | Nucleus                  | MIKC | 0      |
| GbMADS39            | GWHPBAVD019150 | 231         | 26,662.61 | 9.11  | −0.554 | Nucleus                  | MIKC | 6      |
| GbMADS40            | GWHPBAVD021889 | 186         | 21,179.73 | 9.68  | −0.159 | Nucleus                  | MIKC | 1      |
| GbMADS41            | GWHPBAVD021902 | 229         | 26,337    | 8.96  | −0.624 | Nucleus                  | MIKC | 7      |
| GbMADS42            | GWHPBAVD004734 | 356         | 40,514.41 | 6.32  | −0.65  | Nucleus                  | Mα   | 0      |
| GbMADS43            | GWHPBAVD006355 | 277         | 31,917.44 | 8.87  | −0.407 | Nucleus                  | MIKC | 7      |
| GbMADS44            | GWHPBAVD006759 | 120         | 13,179.19 | 9.36  | −0.26  | Nucleus                  | MIKC | 1      |
| GbMADS45            | GWHPBAVD008845 | 227         | 26,228.68 | 6.02  | −0.718 | Nucleus                  | MIKC | 6      |
| GbMADS46            | GWHPBAVD009168 | 169         | 19,411.53 | 10.17 | −0.499 | Nucleus                  | Mα   | 0      |

According to the alignment results of MADS domains v2019 and v2021 (Figure S2), N-terminal diversity reflected the differences between different types of MADS-box domains. In addition, type I domains were more variable than type II domains.

The results of the physicochemical properties of GbMADS proteins are shown in Table 1. The GbMADS protein v2019 was between 91 and 445 aa long, and v2021 was between 61 and 451 aa long. Most GbMADS proteins in v2019 (80.77%) and v2021 (70%) were between 100 and 400 aa long. The predicted molecular weights ranged from 10584.23

to 50951.76 kDa (v2019) and 6849.08 to 51348.86 kDa (v2021). The predicted isoelectric points ranged from 4.7 to 10.2 (v2019) and from 5.53 to 10.58 (v2021). The grand average of hydropathicity ranged from  $-0.754$  to  $0.131$  (v2019) and from  $-0.917$  to  $-0.159$  (v2021). Subcellular localization predicted that all the proteins were localized in the nucleus.

## 2.2. Phylogenetic Analysis and Gene Structure of GbMADS

As model organisms, the classification studies of *MADS* genes in poplar and *A. thaliana* are relatively complete. Here, we refer to their classification in the *GbMADS* phylogeny study. Based on the phylogenetic trees (Figure 1), as well as the classification of genes, the *GbMADS* gene families of v2019 and v2021 could all be divided into two categories: type I (8 members in v2019 and 4 members in v2021) and type II (18 members in v2019 and 16 members in v2021). The type I genes were classified into  $M\alpha$  (five members in v2019 and two members in v2021) and  $M\gamma$  (three members in v2019 and two members in v2021). Similarly, the type II genes could be divided into two subfamilies, MIKC (17 members in v2019 and 15 members in v2021) and  $M\delta$  (1 member in v2019 and 1 member in v2021). Overall, there were fewer *GbMADS* proteins than there were in *A. thaliana* and poplar. However, as in poplar and *A. thaliana*, the MIKC subfamily had the most genes. There were more type II *GbMADS* proteins (18 members in v2019 and 16 members in v2021) than type I *GbMADS* proteins (8 members in v2019 and 4 members in v2021), but the *GbMADS* proteins did not have members of the  $M\beta$  subfamily.

## 2.3. Gene Structure and Motif Analysis

The Gene Structure Display Server (GSDS) website was used for the gene structure analysis (Figure 2). For the *GbMADS* genes in genome v2019, six genes had no introns, and the remaining twenty *GbMADS* genes contained 1 to 10 introns (Table 1). With respect to type I genes, except for *GbMADS11* and *GbMADS13*, the rest did not contain introns. Type II *GbMADS* genes mostly contained two to five introns, with an average number (5.5) much greater than that in the type I *GbMADS* genes (0.5).

For the *GbMADS* genes in genome v2021, six genes had no introns, and the remaining fourteen *GbMADS* genes contained 1 to 12 introns (Table 1). Type I genes did not contain introns except for *GbMADS33*. Most type II *GbMADS* genes contained 7 to 12 introns. The average *MADS* gene number (4.25) of type II was much greater than that of type I (0.25).

Furthermore, gene introns with widely different lengths had also become our focus. In type I genes of v2019, both *GbMADS11* and *GbMADS13* had an intron length of 1 kb. Among the type II genes, 55.56% were greater than 15 kb, of which nine genes (*GbMADS03*, *05*, *06*, *08*, *09*, *10*, *15*, *18*, and *20*) had extralong introns ( $\geq 20$  kb). In genome v2021, *GbMADS33* had an intron length of 1 kb. Type II genes had longer introns, and 37.5% were greater than 15 kb, of which five genes (*GbMADS29*, *31*, *39*, *41*, and *45*) had extralong introns ( $\geq 20$  kb). Their introns were much longer than those of other genes.

In summary, the type II genes of both genomes have more introns than the type I genes and are longer in length. Compared with the v2019 genome, the *GbMADS* genes of v2021 have fewer introns and fewer superlong introns.

## 2.4. Interaction Network and Expression Analysis of GbMADS

To determine the biological function and regulatory network of the *GbMADS* proteins, homologous *MADS*-box proteins of *A. thaliana* were used to predict the *GbMADS* protein–protein interaction network (Figure 3). The homology relationship between *A. thaliana* and Ginkgo *MADS* proteins is shown in Table S3. Based on the interaction between genes, 15 *GbMADS* proteins were homologous to 22 *MADS* proteins in *A. thaliana*. They belong to the MIKC subfamily, except for *GbMADS13*, *14*, *16*, *24*, *37*, *42*, and *46*. Most *GbMADS* proteins could interact with 4–12 proteins. Among the *MADS* proteins of *A. thaliana*, *AGL6*, *AGL8*, and *AGL104* are mainly related to the development of flowers; *PI*, *AG*, *AGL61*, and *SEP* are related to the development of female and male gametophytes; and *AGL62* affects early endosperm development.

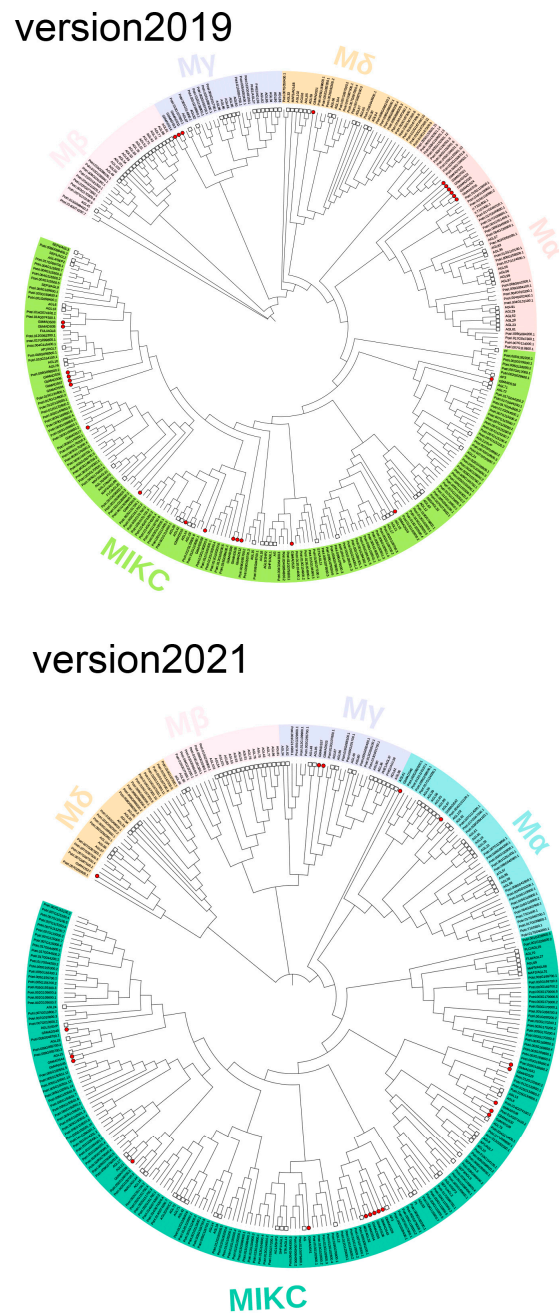
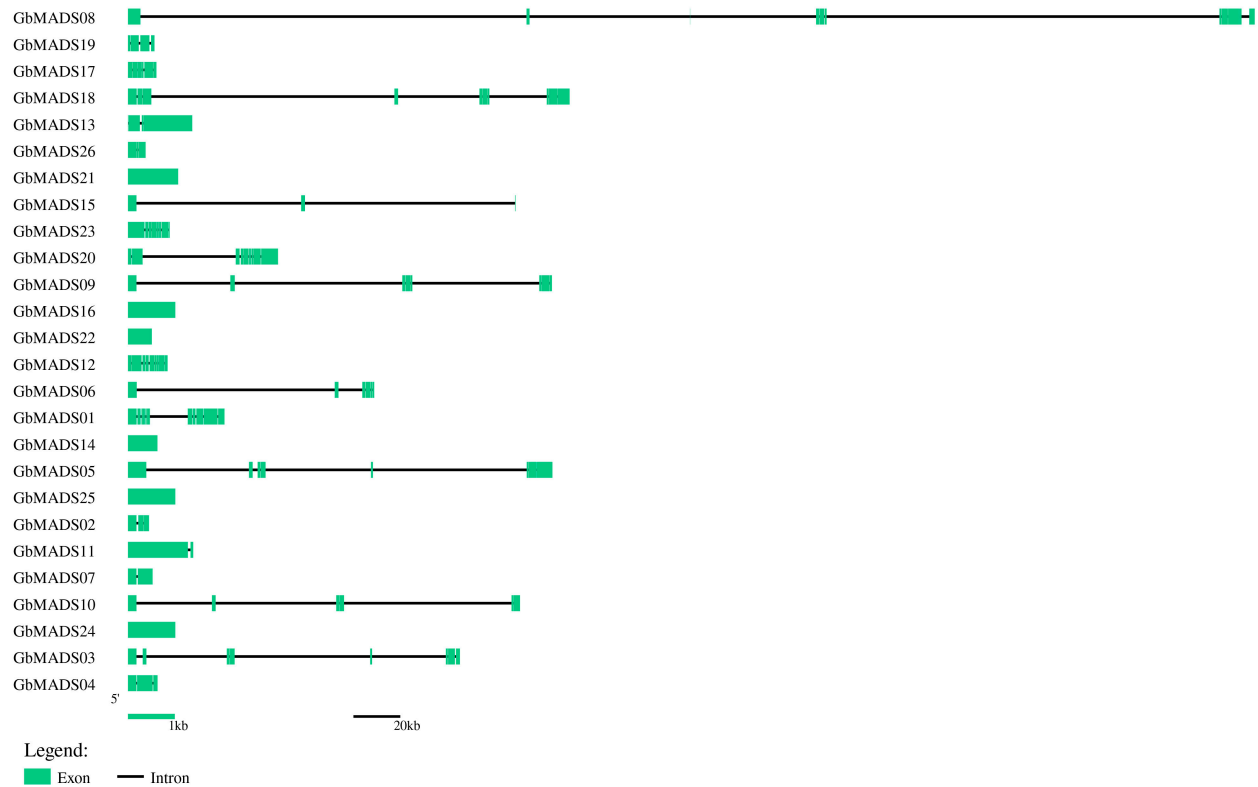


**Figure 1.** A phylogenetic tree was constructed with the ML method, which is composed of homologous MADS protein sequences in Ginkgo, *A. thaliana*, and *Populus L.* The red circle represents MADS in Ginkgo and the white square represents MADS in *A. thaliana*. Version2019 represents the MADS proteins identified from the 2019 version of the genome. Version2021 represents the MADS proteins identified from the 2021 version of the genome. For version2019, the light green represents MIKC subfamily, the dark pink represents  $M\alpha$  subfamily, the light pink represents  $M\beta$  subfamily, the light purple represents  $M\gamma$  subfamily, and the orange represents  $M\delta$  subfamily. For version2021, the green represents MIKC subfamily, the blue represents  $M\alpha$  subfamily, the light pink represents  $M\beta$  subfamily, the light purple represents  $M\gamma$  subfamily, and the light orange represents  $M\delta$  subfamily.

### version 2019



### version2021

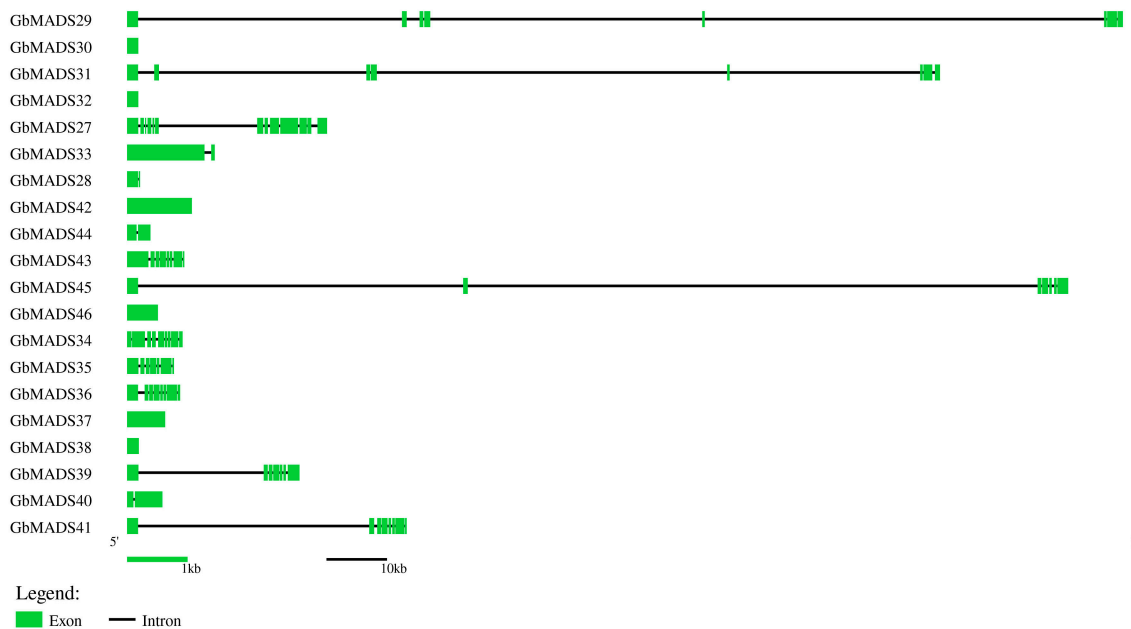


**Figure 2.** Gene structure of *GbMADS* genes. Version2019 represents the *MADS* genes identified from the 2019 version of the genome. Version2021 represents the *MADS* genes identified from the 2021 version of the genome. Green lines are exons, and black lines are introns.

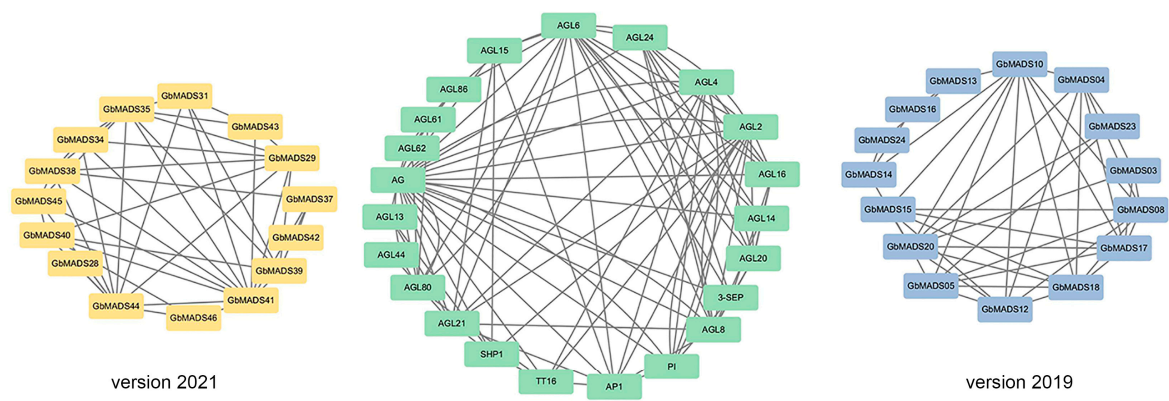


**Figure 3.** Interaction network analysis of GbMADS proteins. Version2019 represents the MADS proteins interaction in the 2019 version of the genome, and Version2021 represents the MADS proteins interaction in the 2021 version of the genome.

Twenty-eight pairs of *GbMADS* genes were selected to explore the expression patterns in eight tissues, namely, female flowers (FF), male flowers (MF), early seeds (ES), developing seeds (DS), mature seeds (MS), roots (R), stems (S), and leaves (L) (Figure 4, Table S4). To avoid duplicate genes, we selected all genes of the 2019 version, as well as genes of the 2021 version with less than 80% similarity to the 2019 version genes (genes with greater than 80% similarity are listed in Table S2).

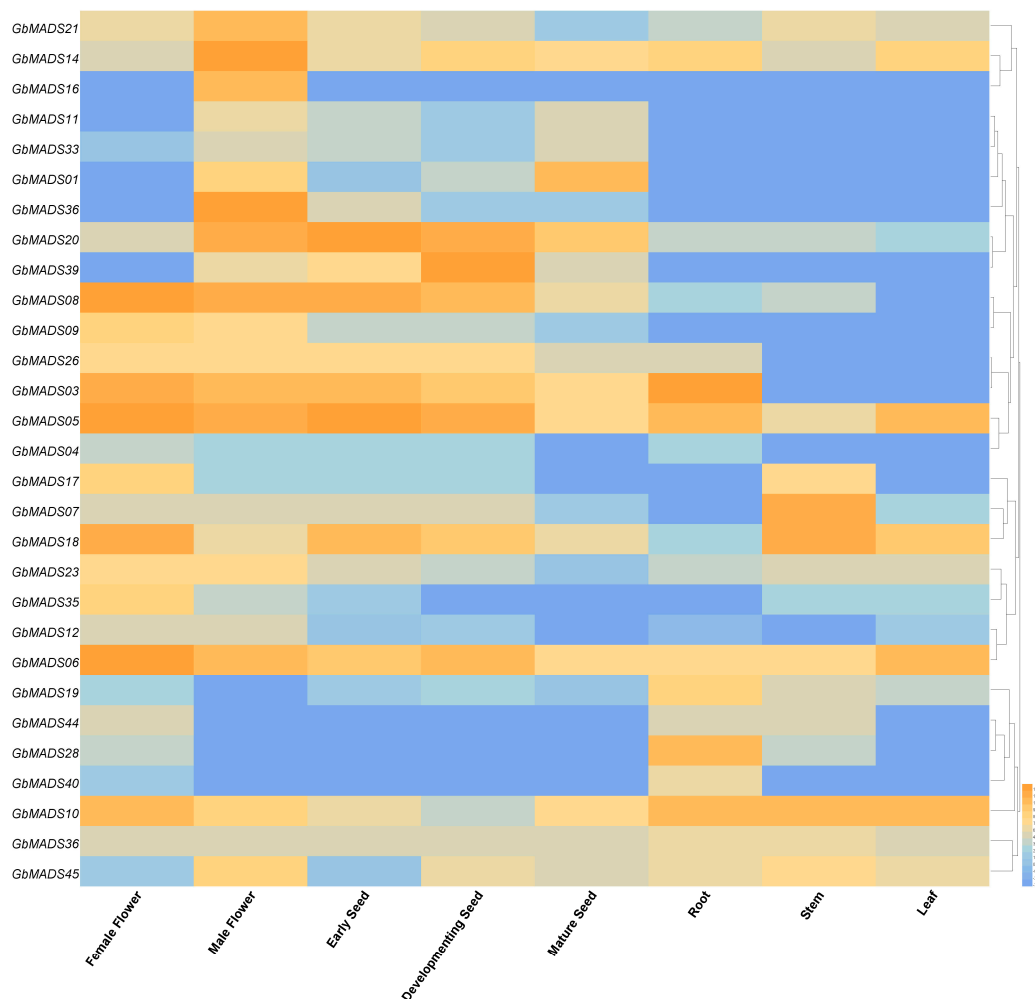


**Figure 4.** *GbMADS* gene expression analysis. Orange to blue represent expression from high to low.

Overall, the most highly expressed genes were in MF and FF, followed by ES and DS. The expression of most genes was low in R, S, and L. Among type I genes, *GbMADS14* showed moderate or high expression in all tissues, with the highest expression in MF, followed by DS. *GbMADS16* and *GbMADS21* were highly expressed in MF and showed moderate or lower expression in other tissues. *GbMADS11* and *GbMADS33* showed low expression in all tissues. Among the type II genes, the M $\delta$  gene *GbMADS01* was most highly expressed in MS, followed by MF. Among the MIKC genes, *GbMADS05*, *06*, and *10* were highly expressed in eight tissues. *GbMADS03*, *20*, *26*, *08*, and *18* were highly expressed in more than half of the tissues, such as FF, MF, ES, DS, and MS. *GbMADS17*, *45*, and *39* were all highly expressed in 2~3 tissues, which were reflected in FF, MF, and DS. *GbMADS23*, *09*, *12*, *36*, *28*, *35*, *36*, *40*, *19*, and *07* were highly expressed in 1~2 tissues, while *GbMADS04* and *GbMADS44* showed low expression in all tissues. In addition, *GbMADS14* in MF, *GbMADS08* in FF, *GbMADS20* in ES, and *GbMADS39* in DS all showed particularly high expression levels. They may play key roles in plant growth and development. In summary, *GbMADS* genes, especially MIKC genes, may play a role in flower organ development and seed development.

### 3. Discussion

#### 3.1. Number and Type of *GbMADS* Proteins

In the genome versions of v2019 and 2021, twenty-six and twenty members of the MADS-box gene family (*GbMADS01* to *GbMADS26* and *GbMADS27* to *GbMADS46*) with complete MADS domains were finally identified, respectively. In a previous study by Yang et al., 26 genes were also identified in the v2019 genome [17]. We found that the number of *GbMADS* proteins was lower than that in most plant species, such as *A. thaliana* (106), poplar (105), and *Salix suchowensis* (60) [3,4,25]. The genomes of these species vary in size (*A. thaliana*, 207 Mb; poplar, 431 Mb; *S. suchowensis*, 356 Mb; Ginkgo, 9.87 Gb). However, the number of protein-coding genes in *A. thaliana* was similar to that in Ginkgo, and those of poplar and *S. suchowensis* were almost twice that in Ginkgo. The Ginkgo genome is large. The increases in genome-wide duplication and repeat sequences increased the size and complexity of the Ginkgo genome. Therefore, gene loss may have occurred frequently throughout the long evolutionary process of Ginkgo.

In reference to the classification of *A. thaliana* and poplar subfamilies for phylogenetic tree construction [3,4], type II genes accounted for a higher proportion of Ginkgo (69.23% and 80% for v2019 and v2021, respectively) than poplar (60.95%) and *Arabidopsis* (47.4%). It has been found that MIKC subfamily genes play important roles in the development of pistils and stamens of gymnosperms [26], suggesting that these genes might play the same role in the sexual differentiation of Ginkgo. Compared with *A. thaliana*, poplar, and other plant species, Ginkgo does not have M $\beta$  genes, and similar results have been found in sesame [27]. This means that the M $\beta$  genes do not play important roles in Ginkgo, as all of them have been lost during evolution.

#### 3.2. Gene Structure of *GbMADS* genes

The expression of genes is related to introns. Different ways in which introns were spliced could result in different activities at different periods, resulting in different proteins. Regardless of v2019 or v2021, the type I *GbMADS* genes had a simple structure. Most of them had zero or only one intron, and they were short (<1 kb). This was similar to the homologs in *A. thaliana*. The type II genes had a higher number of introns and a more variable structure. Some MIKC genes (*GbMADS03*, *05*, *06*, *08*, *09*, *10*, *15*, *18*, *20*, *29*, *31*, *39*, *41*, and *45*) also have extralong introns ( $\geq 20$  kb). Their introns were much longer than the introns of the type II *AtMADS* genes (the longest introns were only 3.8 kb). It has been suggested that the gene expression is richer in genes in which oversized introns and transposons have been inserted [28,29]. These extralong introns indicated that Ginkgo genes are relatively long, and different splicing patterns lead to the diverse expression of genes. It had been confirmed that MIKC genes had a great influence on sex determination

and flower development. [26]. Ginkgo is a dioecious plant species that often takes more than 20 years to distinguish between sexes based on inflorescence characteristics. MIKC genes may have an important influence on the sex determination of Ginkgo, which is important for the early sex distinction of this species.

In addition, we found that the *GbMADS* genes of 2021 version genome had fewer gene introns and were shorter. When we compared the two genomes, we found that the scaffold N50 length of the 2019 version genome was 0.135 Mb, while the scaffold N50 length of the 2021 version genome was 775 Mb [18,19]. N50 is the evaluation index after genome assembly. The longer the length, the better the quality of the assembly. The N50 of the 2021 version is thousands of times higher than that of the 2019 version, indicating that the splicing quality of the 2021 version is better. The incompleteness of gene splicing in different versions of the genome may lead to differences in introns.

### 3.3. Gene Expression and Potential Function

Liao et al. identified nineteen *GbMADS* genes using a combination of transcriptome alignment and de novo prediction and found that the male sex-determining region of Ginkgo contained more than 200 genes. Four *GbMADS* genes that play an important role in sex differentiation were present [30]. According to studies of *A. thaliana*, *AGL80* affects central cell differentiation during female gametophyte development [31], and *AGL61* has a role in female gametophyte development [32]. In this study, we found that type I genes were specifically highly expressed in male flowers. These genes included the *AGL80*-like gene *GbMADS14* and the *AGL61*-like genes *GbMADS16* and *GbMADS21*. Therefore, it is thought that they may play an important role in the sex differentiation of Ginkgo.

In *A. thaliana*, *AGL2* plays a role in floral meristem tissues, thereby ensuring the normal development of petals, stamens, and carpels [33,34]. *AGL6* and *AGL16* were involved in the gene regulation and regulation of long-day flowering time during the development of peanut meristem tissue [35,36], respectively. *AGL20* affected the flowering and developmental period of *A. thaliana* [37]. Zhi Feng et al. found that the expression level of the *SOC1* homolog *Gb01884* varied from low to high in the early stage of flower bud differentiation and emergence, which was based on transcriptome data from Ginkgo [38]. In this study, most of the MIKC subfamily genes were specifically highly expressed in female flowers. Therefore, the *AGL2*-like gene *GbMADS05* might have an effect on the sex determination mechanism of Ginkgo. The *AGL6*-like genes *GbMADS06* and *GbMADS09*, the *AGL16*-like gene *GbMADS17*, and the *AGL20*-like gene *GbMADS08* may regulate the differentiation of female flower buds of Ginkgo.

MIKC genes were also highly expressed in other tissues. *AGL24* (*SOC1*) is a transcriptional activator that promotes the growth of apical meristem tissue [39]. The *AGL24*-like gene *GbMADS18* exhibited a high level of expression at the ends of the stems, which might promote the growth of apical meristem tissue. In addition, we found that MIKC genes exhibited moderate or high expression in young and developing seeds. Lovisetto et al. overexpressed the *AG* homologous gene in Ginkgo and demonstrated that *AG* had a substantial role in the development of fleshy fruits in gymnosperms [40]. This is important for the evolution of seed propagation. *TT16* is involved in the developmental regulation of the endothelium and in the accumulation of proanthocyanidins or condensed tannins, which give the seed its brown pigmentation after oxidation [41]. The *AG*-like gene *GbMADS20* and *TT16*-like gene *GbMADS39* in this study may also play the same role in Ginkgo seeds. When the results of the analysis of the protein interaction networks and gene expression are combined, *GbMADS* genes may be considered to have some impact on the development of reproductive organs and sex determination. It may benefit from further development in the future.

## 4. Materials and Methods

### 4.1. Identification and Phylogenetic Analysis of GbMADS Proteins

The two Ginkgo genomic datasets were accessible at <http://gigadb.org/dataset/100613#> (accessed on 20 January 2022) and <https://ginkgo.zju.edu.cn/genome/> (accessed on 21 January 2022). From the TAIR database (<http://www.arabidopsis.org/>) (accessed on 21 January 2022), we downloaded the MADS-box protein sequences of *A. thaliana*. Then, we aligned them to protein sequences of Ginkgo. The HMMER version 3.0 program was also applied for the Ginkgo MADS-box protein search with the Pfam accession PF00319 [42].

We verified the protein further through the SMART website (<http://smart.embl-heidelberg.de/>) [43] and CDD Database (<https://www.ncbi.nlm.nih.gov/Structure/cdd/wrpsb.cgi>) (accessed on 25 January 2022). Moreover, the MADS-box protein characteristics and subcellular location predictions were determined and carried out using ExPASy (<https://web.expasy.org/protparam/>) and Plant-mPLoc (<http://www.csbio.sjtu.edu.cn/bioinf/plant-multi/>) (accessed on 11 February 2022), respectively.

### 4.2. Sequence Alignment and Phylogenetic Analysis

The Weblogo website (<http://weblogo.berkeley.edu/logo.cgi>) was applied for the GbMADS logos [44]. At the same time, ClustalX version 2.1 and ESPript website (<https://esprpt.ibcp.fr/ESPript/cgi-bin/ESPript.cgi>) (accessed on 18 February 2022) were applied for sequence alignment and for coloring the results of GbMADS in the two versions of the genome.

MEGA 11.0 was used to construct the phylogenetic tree of three species: Ginkgo, populus, and *A. thaliana* [45]. MADS-box protein sequences of *Populus trichocarpa* were acquired from <https://phytozome-next.jgi.doe.gov/> (accessed on 21 January 2022). The results were visualized using the iTOLs online tool (<https://itol.embl.de/itol.cgi>) (accessed on 25 February 2023).

### 4.3. Gene Structure and Protein–Protein Interaction Network Analysis

The exon/intron map was constructed in the GSDS online tool (<http://gsds.gao-lab.org/>) (accessed on 12 May 2023).

A homology analysis of MADS-box proteins in Ginkgo and *A. thaliana* was developed using String online tools (<https://string-db.org/>) (accessed on 11 March 2023). The results were visualized with Cytoscape v3.9.1.

### 4.4. Plant Tissues and Quantitative Analysis

The plant materials were obtained from Nanjing Forestry University (32°4′ N, 118°48′ E). Young seeds, developing seeds, and mature seeds were collected in August, September, and October 2022, respectively. Female flowers, male flowers, roots, stems, and leaves were collected in July 2022. Three different biological replicates were collected for each tissue. After they were sampled, the tissue samples were placed in liquid nitrogen, frozen, and then stored at −80 °C. We converted the results of the quantitative experiments into data and used Heml 1.0 to visualize the expression results.

## 5. Conclusions

For the first time, this study identified 26 and 20 *GbMADS* genes from two Ginkgo genomes, and they could be divided into types I and II. Compared with *A. thaliana*, Ginkgo had fewer *MADS-box* genes, but its genes had more introns and were longer. The oversized introns of the MIKC genes might be an indicator of higher gene expression. Furthermore, through qPCR, it was found that the type I *GbMADS* genes had a certain effect on the development of male flowers, whereas most of the type II *GbMADS* genes affected the development process of female flowers. In addition, genes of the MIKC subfamily might play important roles in the development of young seeds. Taken together, the results showed that *GbMADS* genes not only had an effect on the sex determination mechanism of Ginkgo but also participated in regulating reproduction. The results of this study are conducive

to a better understanding of the structure–function relationship between *MADS-box* gene family members. This study lays an important foundation for exploring the molecular mechanism underlying Ginkgo sex determination.

**Supplementary Materials:** The following supporting information can be downloaded at <https://www.mdpi.com/article/10.3390/plants12183334/s1>. Table S1. Gene ID of more than 80% similarity. Table S2. Primer sequence of GbMADS genes. Table S3. GbMADS genes information homologous to MADS in *Arabidopsis thaliana*. Table S4. Expression of GbMADS genes. Figure S1. Weblogo of GbMADS domain. Figure S2. GbMADS domain sequence alignment. S1. GbMADS protein sequences of v2019 genome. S2. GbMADS protein sequences of v2021 genome.

**Author Contributions:** Conceptualization, P.Z. and Q.Z.; methodology, P.Z.; software, Z.W.; formal analysis, Z.W.; investigation, Y.L.; resources, Y.L.; data curation, P.Z.; writing—original draft preparation, P.Z.; writing—review and editing, P.Z.; visualization, P.Z.; supervision, Q.Z.; project administration, Q.Z.; funding acquisition, Q.Z. All authors have read and agreed to the published version of the manuscript.

**Funding:** This research was funded by the National Natural Science Foundation of China (31902064), Special Project for Research Institute of Zhejiang Province (2021F1065-1), Postgraduate Research & Practice Innovation Program of Jiangsu Province (KYCX22\_1112), and the Priority Academic Program Development of Jiangsu Higher Education Institutions (PAPD).

**Data Availability Statement:** Not applicable.

**Acknowledgments:** We thank Jing Guo for collecting the plant tissues for us.

**Conflicts of Interest:** The authors declare no conflict of interest.

## References

- Messenguy, F.; Dubois, E. Role of MADS-box proteins and their cofactors in combinatorial control of gene expression and cell development. *Gene* **2003**, *316*, 1–21. [[CrossRef](#)] [[PubMed](#)]
- Krizek, B.A.; Fletcher, J.C. Molecular mechanisms of flower development: An armchair guide. *Nat. Rev. Genet.* **2005**, *6*, 688–698. [[CrossRef](#)] [[PubMed](#)]
- Parenicova, L.; de Folter, S.; Kieffer, M.; Horner, D.S.; Favalli, C.; Busscher, J.; Cook, H.E.; Ingram, R.M.; Kater, M.M.; Davies, B.; et al. Molecular and phylogenetic analyses of the complete MADS-box transcription factor family in Arabidopsis: New openings to the MADS world. *Plant Cell* **2003**, *15*, 1538–1551. [[CrossRef](#)] [[PubMed](#)]
- Leseberg, C.H.; Li, A.; Kang, H.; Duvall, M.; Mao, L. Genome-wide analysis of the MADS-box gene family in *Populus trichocarpa*. *Gene* **2006**, *378*, 84–94. [[CrossRef](#)]
- Arora, R.; Agarwal, P.; Ray, S.; Singh, A.K.; Singh, V.P.; Tyagi, A.K.; Kapoor, S. MADS-box gene family in rice: Genome-wide identification, organization and expression profiling during reproductive development and stress. *BMC Genom.* **2007**, *8*, 242. [[CrossRef](#)]
- Smaczniak, C.; Immink, R.G.; Angenent, G.C.; Kaufmann, K. Developmental and evolutionary diversity of plant MADS-domain factors: Insights from recent studies. *Development* **2012**, *139*, 3081–3098. [[CrossRef](#)]
- Kuo, M.H.; Nadeau, E.T.; Grayhack, E.J. Multiple phosphorylated forms of the *Saccharomyces cerevisiae* Mcm1 protein include an isoform induced in response to high salt concentrations. *Mol. Cell. Biol.* **1997**, *17*, 819–832. [[CrossRef](#)]
- Wei, B.; Cai, T.; Zhang, R.; Li, A.; Huo, N.; Li, S.; Gu, Y.Q.; Vogel, J.; Jia, J.; Qi, Y.; et al. Novel microRNAs uncovered by deep sequencing of small RNA transcriptomes in bread wheat (*Triticum aestivum* L.) and *Brachypodium distachyon* (L.) Beauv. *Funct. Integr. Genom.* **2009**, *9*, 499–511. [[CrossRef](#)]
- Wei, B.; Zhang, R.-Z.; Guo, J.-J.; Liu, D.-M.; Li, A.-L.; Fan, R.-C.; Mao, L.; Zhang, X.-Q. Genome-wide analysis of the MADS-box gene family in *Brachypodium distachyon*. *PLoS ONE* **2014**, *9*, e84781. [[CrossRef](#)]
- Ma, J.-J.; Chen, X.; Song, Y.-T.; Zhang, G.-F.; Zhou, X.-Q.; Que, S.-P.; Mao, F.; Pervaiz, T.; Lin, J.-X.; Li, Y.; et al. MADS-box transcription factors *MADS11* and *DAL1* interact to mediate the vegetative-to-reproductive transition in pine. *Plant Physiol.* **2021**, *187*, 247–262. [[CrossRef](#)]
- Liu, Y.; Wang, S.; Li, L.; Yang, T.; Dong, S.; Wei, T.; Wu, S.; Liu, Y.; Gong, Y.; Feng, X.; et al. The Cycas genome and the early evolution of seed plants. *Nat. Plants* **2022**, *8*, 389–401. [[CrossRef](#)] [[PubMed](#)]
- Gramzow, L.; Theissen, G. A hitchhiker’s guide to the MADS world of plants. *Genome Biol.* **2010**, *11*, 214. [[CrossRef](#)] [[PubMed](#)]
- De Bodt, S.; Raes, J.; Florquin, K.; Rombauts, S.; Rouze, P.; Theissen, G.; Van de Peer, Y. Genome-wide structural annotation and evolutionary analysis of the type I MADS-box genes in plants. *J. Mol. Evol.* **2003**, *56*, 573–586. [[CrossRef](#)] [[PubMed](#)]
- Kaufmann, K.; Melzer, R.; Theissen, G. MIKC-type MADS-domain proteins: Structural modularity, protein interactions and network evolution in land plants. *Gene* **2005**, *347*, 183–198. [[CrossRef](#)]

15. Gong, W.; Chen, C.; Dobes, C.; Fu, C.X.; Koch, M.A. Phylogeography of a living fossil: Pleistocene glaciations forced *Ginkgo biloba* L. (Ginkgoaceae) into two refuge areas in China with limited subsequent postglacial expansion. *Mol. Phylogenetics Evol.* **2008**, *48*, 1094–1105. [[CrossRef](#)]
16. Wang, H.Y.; Zhang, Y.Q. The main active constituents and detoxification process of *Ginkgo biloba* seeds and their potential use in functional health foods. *J. Food Compos. Anal.* **2019**, *83*, 103247. [[CrossRef](#)]
17. Yang, K.; Liu, Z.; Chen, X.; Zhou, X.; Ye, J.; Xu, F.; Zhang, W.; Liao, Y.; Yang, X.; Wang, Q. Genome-Wide Identification and Expression Analysis of the MADS-Box Family in *Ginkgo biloba*. *Forests* **2022**, *13*, 1953. [[CrossRef](#)]
18. Guan, R.; Zhao, Y.; Zhang, H.; Fan, G.; Liu, X.; Zhou, W.; Shi, C.; Wang, J.; Liu, W.; Liang, X.; et al. Draft genome of the living fossil *Ginkgo biloba*. *Gigascience* **2016**, *5*, s13742-016. [[CrossRef](#)]
19. Liu, H.; Wang, X.; Wang, G.; Cui, P.; Wu, S.; Ai, C.; Hu, N.; Li, A.; He, B.; Shao, X.; et al. The nearly complete genome of *Ginkgo biloba* illuminates gymnosperm evolution. *Nat. Plants* **2021**, *7*, 748–756. [[CrossRef](#)]
20. Jager, M.; Hassanin, A.; Manuel, M.; Guyader, H.L.; Deutsch, J. MADS-box genes in *Ginkgo biloba* and the evolution of the AGAMOUS family. *Mol. Biol. Evol.* **2003**, *20*, 842–854. [[CrossRef](#)]
21. Xiao, W.; Cheng, J.; Feng, X.; Xing, L.; Zhang, W.; Yong, L.; Cheng, S.; Li, X. Molecular cloning and expression analysis of a MADS-Box gene (*GbMADS2*) from *Ginkgo biloba*. *Not. Bot. Horti Agrobot. Cluj-Napoca* **2015**, *43*, 19–24.
22. Yang, F.; Xu, F.; Wang, X.; Liao, Y.; Chen, Q.; Meng, X. Characterization and functional analysis of a MADS-box transcription factor gene (*GbMADS9*) from *Ginkgo biloba*. *Sci. Horti* **2016**, *212*, 104–114. [[CrossRef](#)]
23. Niu, S.; Li, J.; Bo, W.; Yang, W.; Zuccolo, A.; Giacomello, S.; Chen, X.; Han, F.; Yang, J.; Song, Y.; et al. The Chinese pine genome and methylome unveil key features of conifer evolution. *Cell* **2021**, *185*, 204–217. [[CrossRef](#)]
24. Zheng, Y.; Jiao, C.; Sun, H.; Rosli, H.G.; Pombo, M.A.; Zhang, P.; Banf, M.; Dai, X.; Martin, G.B.; Giovannoni, J.J.; et al. iTAK: A program for genome-wide prediction and classification of plant transcription factors, transcriptional regulators, and protein kinases. *Mol. Plant Breed.* **2016**, *9*, 1667–1670. [[CrossRef](#)] [[PubMed](#)]
25. Qu, Y.; Bi, C.; He, B.; Ye, N.; Yin, T.; Xu, L.-A. Genome-wide identification and characterization of the MADS-box gene family in *Salix suchowensis*. *PeerJ* **2019**, *7*, e8019. [[CrossRef](#)]
26. Wang, D.; Hao, Z.; Long, X.; Wang, Z.; Zheng, X.; Ye, D.; Peng, Y.; Wu, W.; Hu, X.; Wang, G.; et al. The Transcriptome of *Cunninghamia lanceolata* male/female cone reveal the association between MIKC MADS-box genes and reproductive organs development. *BMC Plant Biol.* **2020**, *20*, 508. [[CrossRef](#)]
27. Wei, X.; Wang, L.; Yu, J.; Zhang, Y.; Li, D.; Zhang, X. Genome-wide identification and analysis of the MADS-box gene family in sesame. *Gene* **2015**, *569*, 66–76. [[CrossRef](#)]
28. Korb, M.; Ke, Y.; Johnson, L.F. Stimulation of gene expression by introns: Conversion of an inhibitory intron to a stimulatory intron by alteration of the splice donor sequence. *Nucleic Acids Res.* **1993**, *21*, 5901–5908. [[CrossRef](#)]
29. Vain, P.; Finer, K.R.; Engler, D.E.; Pratt, R.C.; Finer, J.J. Intron-mediated enhancement of gene expression in maize (*Zea mays* L.) and bluegrass (*Poa pratensis* L.). *Plant Cell Rep.* **1996**, *15*, 489–494. [[CrossRef](#)]
30. Liao, Q.; Du, R.; Gou, J.; Guo, L.; Shen, H.; Liu, H.; Nguyen, J.K.; Ming, R.; Yin, T.; Huang, S.; et al. The genomic architecture of the sex-determining region and sex-related metabolic variation in *Ginkgo biloba*. *Plant J.* **2020**, *104*, 1399–1409. [[CrossRef](#)]
31. Portereiko, M.F.; Lloyd, A.; Steffen, J.G.; Punwani, J.A.; Otsuga, D.; Drews, G.N. *AGL80* is required for central cell and endosperm development in Arabidopsis. *Plant Cell* **2006**, *18*, 1862–1872. [[CrossRef](#)] [[PubMed](#)]
32. Steffen, J.G.; Kang, I.H.; Portereiko, M.F.; Lloyd, A.; Drews, G.N. *AGL61* interacts with *AGL80* and is required for central cell development in Arabidopsis. *Plant Physiol.* **2008**, *148*, 259–268. [[CrossRef](#)] [[PubMed](#)]
33. Flanagan, C.A.; Ma, H. Spatially and temporally regulated expression of the MADS-box gene *AGL2* in wild-type and mutant Arabidopsis flowers. *Plant Mol. Biol.* **1994**, *26*, 581–595. [[CrossRef](#)] [[PubMed](#)]
34. Favaro, R.; Pinyopich, A.; Battaglia, R.; Kooiker, M.; Borghi, L.; Ditta, G.; Yanofsky, M.F.; Kater, M.M.; Colombo, L. MADS-box protein complexes control carpel and ovule development in Arabidopsis. *Plant Cell* **2003**, *15*, 2603–2611. [[CrossRef](#)] [[PubMed](#)]
35. Koo, S.C.; Bracko, O.; Park, M.S.; Schwab, R.; Chun, H.J.; Park, K.M.; Seo, J.S.; Grbic, V.; Balasubramanian, S.; Schmid, M.; et al. Control of lateral organ development and flowering time by the Arabidopsis thaliana MADS-box Gene AGAMOUS-LIKE6. *Plant J.* **2010**, *62*, 807–816. [[CrossRef](#)]
36. Hu, J.Y.; Zhou, Y.; He, F.; Dong, X.; Liu, L.Y.; Coupland, G.; Turck, F.; de Meaux, J. miR824-regulated AGAMOUS-LIKE16 contributes to flowering time repression in Arabidopsis. *Plant Cell* **2014**, *26*, 2024–2037. [[CrossRef](#)]
37. Lee, H.; Suh, S.-S.; Park, E.; Cho, E.; Ahn, J.H.; Kim, S.-G.; Lee, J.S.; Kwon, Y.M.; Lee, I. The AGAMOUS-LIKE20 MADS domain protein integrates floral inductive pathways in Arabidopsis. *Genes Dev.* **2000**, *14*, 2366–2376. [[CrossRef](#)]
38. Feng, Z.; Yang, T.; Li, M.; Dong, J.; Wang, G.; Wang, Q.; Wang, Y. Identification and cloning of *GbMADS6*, a *SOC1* homolog gene involved in floral development in *Ginkgo biloba*. *J. Plant Biochem. Biotechnol.* **2021**, *30*, 554–563. [[CrossRef](#)]
39. Gregis, V.; Sessa, A.; Colombo, L.; Kater, M.M. *AGL24*, *SHORT VEGETATIVE PHASE*, and *APETALA1* redundantly control AGAMOUS during early stages of flower development in Arabidopsis. *Plant Cell* **2006**, *18*, 1373–1382. [[CrossRef](#)]
40. Lovisetto, A.; Baldan, B.; Pavanello, A.; Casadoro, G. Characterization of an AGAMOUS gene expressed throughout development of the fleshy fruit-like structure produced by *Ginkgo biloba* around its seeds. *BMC Evol. Biol.* **2015**, *15*, 139. [[CrossRef](#)]
41. Erdmann, R.; Gramzow, L.; Melzer, R.; Theißen, G.; Becker, A. *GORDITA* (*AGL63*) is a young paralog of the Arabidopsis thaliana B-sister MADS box gene *ABS* (*TT16*) that has undergone neofunctionalization. *Plant J.* **2010**, *63*, 914–924. [[CrossRef](#)] [[PubMed](#)]

42. Finn, R.D.; Mistry, J.; Schuster-Böckler, B.; Griffiths-Jones, S.; Hollich, V.; Lassmann, T.; Moxon, S.; Marshall, M.; Khanna, A.; Durbin, R.; et al. Pfam: Clans, web tools and services. *Nucleic Acids Res.* **2006**, *34*, 247–251. [[CrossRef](#)] [[PubMed](#)]
43. Larkin, M.A.; Blackshields, G.; Brown, N.P.; Chenna, R.; McGettigan, P.A.; McWilliam, H.; Valentin, F.; Wallace, I.M.; Wilm, A.; Lopez, R.; et al. Clustal W and Clustal X version 2.0. *Bioinformatics* **2007**, *23*, 2947–2948. [[CrossRef](#)] [[PubMed](#)]
44. Crooks, G.E.; Hon, G.; Chandonia, J.M.; Brenner, S.E. WebLogo: A sequence logo generator. *Genome Res.* **2004**, *14*, 1188–1190. [[CrossRef](#)]
45. Edgar, R.C. MUSCLE: A multiple sequence alignment method with reduced time and space complexity. *BMC Bioinform.* **2004**, *5*, 113. [[CrossRef](#)]

**Disclaimer/Publisher’s Note:** The statements, opinions and data contained in all publications are solely those of the individual author(s) and contributor(s) and not of MDPI and/or the editor(s). MDPI and/or the editor(s) disclaim responsibility for any injury to people or property resulting from any ideas, methods, instructions or products referred to in the content.